Deep Knowledge-Infused Transformer for NSCLC Lymph Node Station Metastasis Prediction: Development of an AI-Powered Intraoperative Decision System

Jie Zhao[1,2,*], Zifan Chen[3,5,1*], Guangzhengao Yang[3], Yijiang He[1], Li Zhang[3], and Bin Dong[4,5,1]

[1] PKU-Changsha Institute for Computing and Digital Economy, Changsha, China
[2] National Engineering Laboratory for Big Data Analysis and Applications, Peking University, Beijing, China
[3] Center for Data Science, Peking University, Beijing, China
[4] Beijing International Center for Mathematical Research and the New Cornerstone Science Laboratory, Peking University, Beijing, China
[5] Center for Machine Learning Research, Peking University, Beijing, China
jiezhao@pku.edu.cn

Abstract. Non-small cell lung cancer (NSCLC) is one of the leading causes of cancer-related mortality, with lymph node metastasis serving as a critical factor in both prognosis and treatment decisions. Lymph node station (LNS) dissection is an essential procedure in the management of NSCLC patients; however, over-dissection may expose patients to unnecessary risks, while under-dissection could lead to undetected metastases. Despite its importance, predicting the exact metastasis status during surgery remains challenging. To address this challenge and meet the urgent need in clinical practice, this study presents the Deep Knowledge-infused Transformer (DKiT) model, designed to predict LNS metastasis in previously unexamined regions by capturing the relationships between LNSs. Furthermore, DKiT is augmented with clinical prior knowledge through a multi-stage infusion mechanism during the decoding phase, enhancing both model performance and interpretability. Additionally, we developed an AI-powered intraoperative decision support system based on DKiT, which provides real-time surgical recommendations informed by frozen pathology results. Experimental results show that DKiT achieves an AUC score of 0.812 for LNS-level metastasis prediction, outperforming other comparative methods. The clinical system achieves a recall of 0.930 and precision of 0.865 in the retrospective cohort collected from collaborating hospitals, highlighting its potential in guiding NSCLC treatment decisions. The source code is available at https://github.com/czifan/DKiT.

Keywords: Lymph node metastasis · Non-small cell lung cancer · Deep learning · Intraoperative decision system.

*Equal contribution. Work done during Zifan Chen's internship at PKU-Changsha Institute for Computing and Digital Economy.

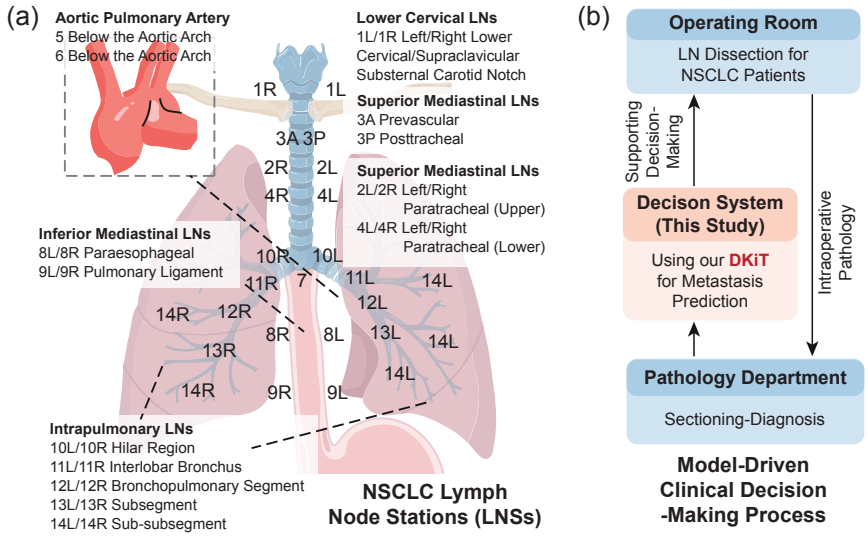

Fig. 1. Overview of Lymph Node Stations in NSCLC (a) and the AI-Powered Decision Support System for Intraoperative Use (b).

1 Introduction

Non-small cell lung cancer (NSCLC) remains one of the leading causes of cancer-related mortality worldwide [5], with lymph node (LN) metastasis playing a critical role in both prognosis [12] and treatment decisions [18]. In clinical practice, LN dissection is a central component of NSCLC treatment [22]. However, both excessive and inadequate dissection can have substantial consequences for patients. Over-extensive dissection may subject patients to unnecessary surgical risks, while insufficient dissection may leave metastases undetected, potentially leading to disease progression. To enhance the prediction of LN metastasis, clinical staging methods are often supplemented with intraoperative imaging or frozen pathology examinations to assess the metastasis status of unexamined LNs. However, these rule-based methods often fail to capture the complex and individualized metastatic patterns of LNSs, particularly the interrelationships between different LNs or lymph node stations (LNSs, as defined in Figure 1(a)).

In recent years, the rapid development of deep learning techniques has opened new avenues for addressing this challenge in the medical field [21,8,19,13]. Deep learning models, particularly Transformer-based models, have shown considerable success in medical image analysis [15,9,23], clinical decision support [2,11], and disease prediction [17,4]. The attention mechanism in Transformer models makes them particularly effective in modeling complex relationships between clinical objects. For instance, He et al. proposed using Transformer models to model the metastatic relationships between source and target lesions in series of CT images [6]; Lu et al. applied Transformer models to capture the interconnec-

tions between different tissue regions in H&E pathology whole-slide images [14]; and several studies [20,1,7] treated longitudinal patient follow-up data from multiple time points as distinct objects, employing Transformer models to explore the temporal dynamics of such data. These studies highlight the powerful and robust ability of Transformer models to capture complex relationships between clinical objects. However, there has been no exploration into the use of advanced AI technologies, such as Transformers, to describe the metastatic relationships between LNSs. Effectively modeling these relationships could have important clinical implications. For example, based on intraoperative frozen pathology results, the next LNS that needs to be dissected could be real-time predicted, minimizing unnecessary surgical interventions and improving intraoperative diagnostic efficiency, ultimately enhancing patient outcomes (as shown in Figure 1(b)).

Against this backdrop and the urgent need in clinical practice, we propose a Deep Knowledge-infused Transformer model (DKiT), for predicting LNS metastasis in NSCLC patients. The main contributions of this study are as follows:

1. We propose a Transformer-based framework for predicting LNS metastasis, enabling accurate identification of high-risk LNSs based on existing metastasis information within the patient.
2. We introduce a clinical knowledge infusion mechanism to markedly enhance the model's understanding of LNS metastasis by injecting encoded prior knowledge through graph learning during the decoding phase.
3. We further develop an AI-powered system based on the DKiT, providing real-time recommendations for the next LNSs to be dissected and improving clinical decision-making.
4. We evaluate the DKiT and system by collecting a real data cohort of 919 NSCLC cases, demonstrating a 5.45% improvement in LNS metastasis prediction accuracy compared to existing methods, with a recall improvement ranging from 2.20% to 8.75% in system decision-making across various clinical parameter settings, underscoring its accuracy and clinical relevance.

2 Methods

The primary objective of this study is to develop a model for predicting LNS metastasis in NSCLC patients and to establish a clinical decision support system. This process involves two key steps: first, constructing a metastasis prediction model based on cross-LNS relationships, and then developing an AI-powered decision support system utilizing the trained prediction model. As illustrated in Figure 2, the input to the prediction model includes the current metastasis status of LNSs. The model consists of two primary branches. The first branch formalizes the clinical prior knowledge regarding the relationships between different LNSs into a graph structure, where each LNS is represented as a node and their adjacent relationships (i.e. 1L and 2L are spatial neighbors; Figure 1(a)) are represented as edges. A graph-based encoder is employed to extract embeddings

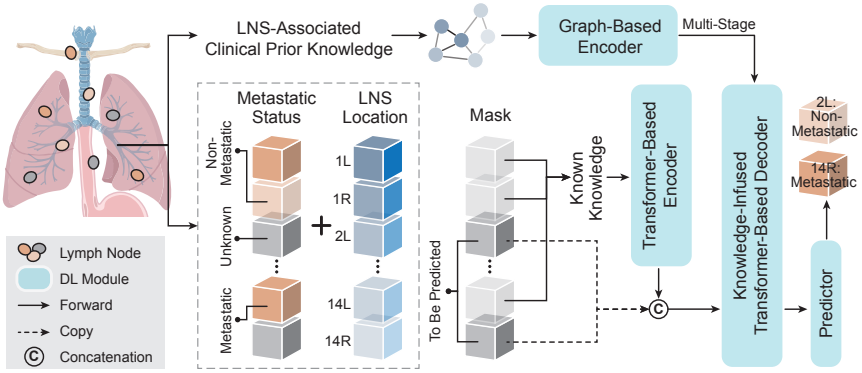

Fig. 2. Architecture of the Proposed DKiT Model for LNS Metastasis Prediction.

for each LNS (denoted as $\mathbf{G} \in \mathbb{R}^{N_{\text{LNS}} \times C}$). The second branch decodes information, such as the metastasis status and location of LNSs, through embeddings (denoted as $\mathbf{M} \in \mathbb{R}^{N_{\text{LNS}} \times C}$ and $\mathbf{L} \in \mathbb{R}^{N_{\text{LNS}} \times C}$, respectively). These embeddings are then used to model the relationships between multiple LNSs using a Transformer-based architecture. During the decoding phase, clinical knowledge is injected through multi-stage graph-based embeddings, and a predictor forecasts the metastasis status of unexamined LNSs. The following sections provide a detailed description of these modules.

2.1 Transformer-Based Prediction Architecture

The metastasis status and LNS location information are encoded and combined into a unified representation, denoted as $\mathbf{X} = \mathbf{M} + \mathbf{L} \in \mathbb{R}^{N_{\text{LNS}} \times C}$. Additionally, a "Mask" indictor ($\mathbf{M}_{\text{mask}} \in \{0,1\}^{N_{\text{LNS}}}$) is constructed, identifying LNSs that require prediction (with a value of 1) and those that are known (with a value of 0). For the known LNSs, their representations are organized into a matrix $\mathbf{X}_{\text{known}} = \{\mathbf{X}_i\}_{i|\mathbf{M}_{\text{mask},i}=0}$, which serves as the known knowledge and input to the Transformer-based encoder with S_{encoder} stages. The encoder is designed using the standard self-attention mechanism [21], where each module consists of an attention block followed by a feed-forward network (FFN). The output of the encoder, denoted as $\mathbf{H}_{\text{encoder}}$, captures the relationships between the known metastasis status of LNSs. The next step involves concatenating the representations of the unexamined LNSs (whose metastasis status needs to be predicted) with the encoder output, denoted as $\mathbf{H} = [\mathbf{H}^{\text{T}}_{\text{encoder}}, \{\mathbf{X}_j\}^{\text{T}}_{j|\mathbf{M}_{\text{mask},j}=1}]^{\text{T}} \in \mathbb{R}^{N_{\text{LNS}} \times C}$. Then, the graph-based embeddings $\mathbf{G}$ are used for knowledge infusion with $\mathbf{H}$ during multi-stage (S_{decoder}) decoding, providing the final embeddings for the unexamined LNSs, and a Multi-Layer Perceptron (MLP) is used for predictions. During training, the model employs a mask-and-predict strategy, using the known metastasis data as supervisory labels to calculate binary cross-entropy loss, which guides backpropagation and parameter optimization.

2.2 Knowledge Infusion Mechanism

Let the hidden embeddings at the s-th stage in decoding be denoted as $\mathbf{H}_s$, and the corresponding graph embeddings as $\mathbf{G}_s$. Since our method supports the infusion of multiple clinical prior knowledge graphs, we define the set of knowledge graphs as $\{\mathbf{G_{s,k}}\}_{k\in\{1,\cdots,N_{\text{graph}}\}}$. Inspired by previous studies on information infusion [2,3], we treat the hidden embeddings as the primary feature and apply a linear transformation to generate the "Query" ($\mathbf{Q}_s$). Similarly, each graph embedding is linearly transformed to produce the "Key" and "Value" ($\mathbf{K}_{s,k}$ and $\mathbf{V}_{s,k}$). The knowledge infusion is performed as follows:

$$\hat{\mathbf{H}}_s = \text{LayerNorm}\left(\mathbf{H}_s + \sum_{k=1}^{N_{\text{graph}}} \alpha_k \cdot \mathcal{A}(\mathbf{Q}_s, \mathbf{K}_{s,k}, \mathbf{V}_{s,k})\right), \tag{1}$$

where $\mathcal{A}(\mathbf{Q},\mathbf{K},\mathbf{V}) = \text{SoftMax}\left(\frac{\mathbf{Q}\mathbf{K}^{\text{T}}}{\sqrt{C}}\right)\mathbf{V}$ is implemented as cross-attention, and α_k represents a dynamic attention weight to integrate information from multiple graphs, which is computed as a gated attention. Subsequently, the standard attention module and FFN perform relational reasoning between all LNSs. Repeating the knowledge infusion process for S_{decoder} stages completes the decoding procedure.

2.3 AI-Powered Intraoperative Decision Support System

As shown in Figure 1(b), the process begins with the first round of LNS dissection, where frozen samples are sent to the pathology department for diagnosis. Suppose that the metastasis status of N_{init} LNSs is obtained, serving as the initial condition for the system. The trained DKiT is then applied to predict the metastasis statuses of the remaining $N_{\text{LNS}} - N_{\text{init}}$ unexamined LNSs. These predictions are ranked in descending order based on the predicted metastasis scores. The top N_{pred} LNSs with scores exceeding a threshold τ are recommended for further dissection. Afterward, the newly dissected LNSs are sent for intraoperative pathology testing, providing updated information. This newly acquired information is integrated into the system, and the process is repeated iteratively. This cycle continues until the surgery is completed or the model predicts that no further LNSs with high metastasis risk remain. The execution of this iterative procedure forms the AI-powered intraoperative decision support system, providing real-time recommendations for surgical decision-making and optimizing the dissection strategy based on the latest available information.

3 Experiments

3.1 Experimental Settings

Dataset The data for this study were collected from our collaborating hospitals and include systemic LNS dissection data from 919 NSCLC patients, all staged

as N1 or N2. The patients were randomly split into training (733 patients), validation (85), and test (101) sets. Following the surgical guidelines of the National Comprehensive Cancer Network (NCCN), each patient underwent dissection of at least three N2 stations. For patients staged as N2, ipsilateral mediastinal LN dissection was performed, while contralateral LNs were not dissected. Based on the LN location, data for each patient were organized into several LNSs (details are shown in Figure 1(a)). Labels for each LNS are encoded as 0 (no metastasis), 1 (metastasis present), or None (node not dissected).

Implementation Details We utilize Word2Vec [16] to encode metastasis information and LNS locations into embeddings. The dimensionality of all embeddings is $C = 64$, and the hidden size of FFN is 256. N_{encoder} is set to 4 to ensure comprehensive encoding of known knowledge, while N_{decoder} is set to 2 enable faster inference. Dropout with a probability of 0.1 is applied across all layers. A two-layer Graph Convolutional Network [10] (GCN) is used to encode prior knowledge. The model is implemented in PyTorch (v2.0.1) and trained on a single A800 GPU with CUDA (v11.9) and eight 8358P CPUs. We apply the AdamW optimizer with an initial learning rate (LR) of 1×10^{-3}, a weight decay of 1×10^{-4}, and cyclic cosine learning rate decay, reducing the LR to 1×10^{-5} every 100 epochs. The model is trained for 400 epochs with a batch size of 128. We apply Exponential Moving Average (EMA) with a decay factor of 0.99 and utilize early stopping based on validation performance to retain the final model weights. The performance reported below is evaluated on the test set.

Comparison Methods We compare our model with several baseline approaches: 1) Statistical models (S-Model): These methods access the correlation between local and overall LNS status using simple statistics (e.g., mean, mode, percentiles) of known LNS labels. 2) Machine learning models (ML-Model): This category predicts LNS metastasis based on available LNS data using machine learning algorithms (e.g., Decision Trees, SVM, Random Forests). 3) Graph-based models with prior knowledge (G-Model): These models leverage LNS relationships encoded in graph networks to predict the status of unknown LNS. For each category, we report the best-performing model in the following.

Evaluation Metrics We assess prediction accuracy at the LNS level using AUC_{LNS} and evaluate clinical decision support through recall and precision.

3.2 Comparison with Other Methods

As shown in Table 1, the proposed DKiT outperforms other comparison methods both in LNS metastasis prediction and clinical metrics at the patient level. Specifically, DKiT achieves an AUC_{LNS} of 0.812 for LNS metastasis prediction, representing a 5.45% relative improvement over the ML-Model and a 0.102 absolute improvement over the clinically-based G-Model. In simulation settings with varying initial clinical parameters (1/3/5 known LNSs), DKiT consistently maintains high recall rates, improving from 0.833 to 0.930 as more initial information is provided. This high recall rate is crucial in clinical practice, as it indicates a lower likelihood of missing metastatic LNSs, which is often associated

Table 1. Comparison between various models. **Bold** indicates the best performance, while 95% confidence interval in square brackets. ± represents the standard deviation of metrics across patients. ↑ shows the relative improvement over the second-best method.

Metrics	S-Model	ML-Model	G-Model	DKiT$_{\textbf{(Ours)}}$	↑ (%)
AUC_{LNS}	0.555 [.522, .587]	0.770 [.731, .805]	0.710 [.665, .748]	**0.812** [.777, .845]	5.45
			$N_{init} = 1$		
Recall	0.348 ±0.455	0.723 ±0.336	0.766 ±0.314	**0.833** ±0.255	8.75
Precision	0.213 ±0.287	0.551 ±0.339	0.509 ±0.273	**0.597** ±0.274	8.35
			$N_{init} = 3$		
Recall	0.500 ±0.432	0.809 ±0.277	0.828 ±0.273	**0.854** ±0.221	3.14
Precision	0.546 ±0.444	0.708 ±0.306	0.683 ±0.286	**0.744** ±0.271	5.08
			$N_{init} = 5$		
Recall	0.771 ±0.353	0.904 ±0.227	0.910 ±0.204	**0.930** ±0.176	2.20
Precision	0.820 ±0.337	0.807 ±0.268	0.823 ±0.258	**0.865** ±0.231	5.10

with improved patient prognosis. Furthermore, DKiT achieves the highest precision across all experimental groups while maintaining high recall, demonstrating its ability to accurately identify LNSs with a high probability of metastasis. This ensures that unnecessary LNS dissection is minimized, reducing patient risk. Moreover, we observe that the S-Model (based on the most frequent LNS metastasis states) performs poorly with only one known LNS, but its performance improves rapidly as more information becomes available. This suggests that the metastasis state of most LNSs in patients is closely linked to global statistical patterns, highlighting the challenge of predicting finer, patient-specific variations, where the DKiT excels. Notably, even with limited initial LNS information, DKiT maintains strong performance, suggesting its ability to model the semantic relationships across different LNS regions and leverage inter-LNS correlations effectively for accurate prediction.

3.3 Ablation Studies

We conducted ablation experiments to assess the impact of different clinical prior knowledge injections on the DKiT model. We tested the model with no prior knowledge (w/o), with single knowledge (+K1, +K2, +K3), and with all three knowledge injected simultaneously (+K1/K2/K3). K1, K2, and K3 represent clinical knowledge graphs based on anatomic proximity, rule transfer mode, and discovered transfer paradigms, respectively. As shown in Figure 3(a), even without prior knowledge injection, DKiT achieved a high AUC of 0.806 for LNS metastasis prediction. While single knowledge injections had minimal effect on AUC, they did improve recall and precision. This is because the LNS-level prediction task during model development relies on large amounts of known LNS data to predict only one unknown LNS. However, in real-world applications, the model often needs to infer future LNS based on only a small amount of known LNSs. Thus, the injection of prior knowledge improves the model's robustness when operating with limited known information. The simultaneous injection of

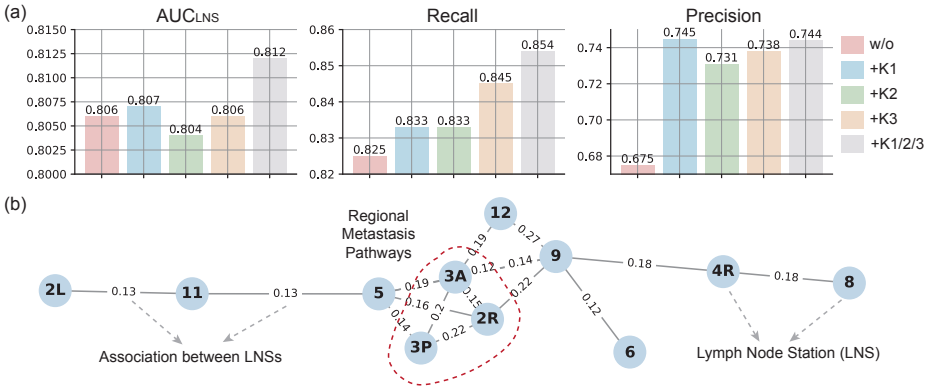

Fig. 3. Ablation study results (a) and correlation analysis of LNSs (b).

all three knowledge resulted in the best overall performance, except for precision, where +K1 performed similarly. This demonstrates DKiT's ability to integrate multiple knowledge sources, and its scalability for future knowledge expansions, such as incorporating new knowledge (K4) into the model.

3.4 LNS Correlation Analysis

We analyze the correlation between LNSs using cosine similarity of their location embeddings **L**. As shown in Figure 3(b), nodes (LNSs) "3A", "2R", "3P", "9", "12", and "5" form a regional metastasis pathway (red dotted box), indicating that tumors in these areas are likely to spread through these connected LNSs. This grouping reflects the anatomical and functional proximity of these nodes, which facilitates metastatic progression. "3A", in particular, plays a pivotal role in NSCLC metastasis. Located near major airways and blood vessels, "3A" serves as a critical junction for early tumor spread. Its high connectivity with adjacent nodes highlights its importance as a key site for metastasis, especially in right-sided NSCLC [24]. In conclusion, embedding models combined with prior knowledge enhance DKiT's understanding of LNS correlations, improving interpretability in the metastasis prediction process.

4 Conclusion

In this study, we introduced the Deep Knowledge-infused Transformer (DKiT) model for predicting LNS metastasis in NSCLC patients. By integrating clinical prior knowledge during the decoding phase, DKiT effectively captures the complex relationships between LNSs and accurately predicts the metastasis status of unexamined LNSs. We further developed an AI-powered intraoperative decision support system that provides real-time recommendations to guide surgical decisions. Retrospective validation of the system demonstrated its ability

to enhance surgical decision-making and predict metastasis in previously unexamined LNs. This work reveals the potential of using Transformer models to model LNS metastasis relationships and the clinical applicability of the model. We acknowledge that the current evaluation was based on a single-center retrospective cohort, which may limit the generalizability of our findings. In future research, we plan to transform this system into software and conduct prospective as well as multi-center studies to further validate its clinical utility. Moreover, we recognize the importance of explicitly incorporating uncertainties and hypothetical LNS statues in future versions of the model to better inform surgical decisions when facing ambiguous or unknown lymph node information.

Disclosure of Interests The authors have no competing interests to declare that are relevant to the content of this article.

Acknowledgements This work was supported by the Municipal Natural Science Foundation (kq2402002) and the National Natural Science Foundation of China (12090022). The anatomical illustrations in Figs. 1 and 2 were adapted from materials provided by Biovisart (`https://biovisart.com.cn`).

References

1. Chen, Q., Fu, Q., Bai, H., Hong, Y.: Longformer: longitudinal transformer for alzheimer's disease classification with structural mris. In: Proceedings of the IEEE/CVF winter conference on applications of computer vision (CVPR). pp. 3575–3584 (2024)
2. Chen, Z., Chen, Y., Sun, Y., Tang, L., Zhang, L., Hu, Y., He, M., Li, Z., Cheng, S., Yuan, J., et al.: Predicting gastric cancer response to anti-her2 therapy or anti-her2 combined immunotherapy based on multi-modal data. Signal Transduction and Targeted Therapy **9**(1), 222 (2024)
3. Chen, Z., Zhao, J., Yu, H., Zhang, Y., Zhang, L.: Multi-scale context-guided lumbar spine disease identification with coarse-to-fine localization and classification. In: 2022 IEEE 19th International Symposium on Biomedical Imaging (ISBI). pp. 1–5. IEEE (2022)
4. Dong, H., Yao, J., Tang, Y., Yuan, M., Xia, Y., Zhou, J., Lu, H., Zhou, J., Dong, B., Lu, L., et al.: Improved prognostic prediction of pancreatic cancer using multi-phase ct by integrating neural distance and texture-aware transformer. In: International Conference on Medical Image Computing and Computer-Assisted Intervention. pp. 241–251. Springer (2023)
5. Gridelli, C., Rossi, A., Carbone, D.P., Guarize, J., Karachaliou, N., Mok, T., Petrella, F., Spaggiari, L., Rosell, R.: Non-small-cell lung cancer. Nature reviews Disease primers **1**(1), 1–16 (2015)
6. He, M., Chen, Z.f., Liu, S., Chen, Y., Zhang, H., Zhang, L., Zhao, J., Yang, J., Zhang, X.t., Shen, L., et al.: Deep learning model based on multi-lesion and time series ct images for predicting the benefits from anti-her2 targeted therapy in stage iv gastric cancer. Insights into Imaging **15**(1), 59 (2024)
7. Holste, G., Lin, M., Zhou, R., Wang, F., Liu, L., Yan, Q., Van Tassel, S.H., Kovacs, K., Chew, E.Y., Lu, Z., et al.: Harnessing the power of longitudinal medical imaging for eye disease prognosis using transformer-based sequence modeling. NPJ Digital Medicine **7**(1), 216 (2024)

8. Isensee, F., Jaeger, P.F., Kohl, S.A., Petersen, J., Maier-Hein, K.H.: nnu-net: a self-configuring method for deep learning-based biomedical image segmentation. Nature methods **18**(2), 203–211 (2021)
9. Karimi, D., Vasylechko, S.D., Gholipour, A.: Convolution-free medical image segmentation using transformers. In: International conference on medical image computing and computer-assisted intervention (MICCAI). pp. 78–88. Springer (2021)
10. Kipf, T.N., Welling, M.: Semi-supervised classification with graph convolutional networks. arXiv preprint arXiv:1609.02907 (2016)
11. Lai, T.: Interpretable medical imagery diagnosis with self-attentive transformers: a review of explainable ai for health care. BioMedInformatics **4**(1), 113–126 (2024)
12. Lee, J.G., Lee, C.Y., Park, I.K., Kim, D.J., Park, S.Y., Kim, K.D., Chung, K.Y.: Number of metastatic lymph nodes in resected non–small cell lung cancer predicts patient survival. The Annals of thoracic surgery **85**(1), 211–215 (2008)
13. Li, H., Wang, Y., Zhu, J., Guo, D., Yu, Q., Yan, K., Lu, L., Ye, X., Zhang, L., Wang, Q., et al.: Semi-supervised lymph node metastasis classification with pathology-guided label sharpening and two-streamed multi-scale fusion. In: International conference on medical image computing and computer-assisted intervention (MICCAI). pp. 623–633. Springer (2024)
14. Lu, M.Y., Williamson, D.F., Chen, T.Y., Chen, R.J., Barbieri, M., Mahmood, F.: Data-efficient and weakly supervised computational pathology on whole-slide images. Nature biomedical engineering **5**(6), 555–570 (2021)
15. Ma, J., He, Y., Li, F., Han, L., You, C., Wang, B.: Segment anything in medical images. Nature Communications **15**(1), 654 (2024)
16. Mikolov, T., Chen, K., Corrado, G., Dean, J.: Efficient estimation of word representations in vector space. arXiv preprint arXiv:1301.3781 (2013)
17. Moor, M., Banerjee, O., Abad, Z.S.H., Krumholz, H.M., Leskovec, J., Topol, E.J., Rajpurkar, P.: Foundation models for generalist medical artificial intelligence. Nature **616**(7956), 259–265 (2023)
18. Prenzel, K.L., Mo, S.P., Sinning, J.M., Baldus, S.E., Brochhagen, H.G., Schneider, P.M., Ho, A.H., et al.: Lymph node size and metastatic infiltration in non-small cell lung cancer. Chest **123**(2), 463–467 (2003)
19. Ronneberger, O., Fischer, P., Brox, T.: U-net: Convolutional networks for biomedical image segmentation. In: International conference on medical image computing and computer-assisted intervention (MICCAI). pp. 234–241. Springer (2015)
20. Sun, Y., Li, K., Chen, D., Hu, Y., Zhang, S.: Lomia-t: A transformer-based longitudinal medical image analysis framework for predicting treatment response of esophageal cancer. In: International conference on medical image computing and computer-assisted intervention (MICCAI). pp. 426–436. Springer (2024)
21. Vaswani, A., Shazeer, N., Parmar, N., Uszkoreit, J., Jones, L., Gomez, A.N., Kaiser, Ł., Polosukhin, I.: Attention is all you need. Advances in neural information processing systems (NeurIPS) **30** (2017)
22. Watanabe, S.i., Asamura, H.: Lymph node dissection for lung cancer: significance, strategy, and technique. Journal of thoracic oncology **4**(5), 652–657 (2009)
23. Yuan, M., Xia, Y., Chen, X., Yao, J., Wang, J., Qiu, M., Dong, H., Zhou, J., Dong, B., Lu, L., et al.: Cluster-induced mask transformers for effective opportunistic gastric cancer screening on non-contrast ct scans. In: International conference on medical image computing and computer-assisted intervention (MICCAI). pp. 146–156. Springer (2023)
24. Zheng, H., Gao, W., Fei, K., Xie, H.k., Jiang, G.n., Ding, J.a., Li, C., Chen, C., Zhang, L.: Prognostic role of station 3a mediastinal nodes for non-small-cell lung cancers. Interactive cardiovascular and thoracic surgery **17**(3), 447–454 (2013)